N93-29366

ANALYSIS OF LDEF MICROMETEOROID/DEBRIS DATA AND DAMAGE TO COMPOSITE MATERIALS

R. C. Tennyson and G. Manuelpillai
University of Toronto Institute for Aerospace Studies
4925 Dufferin Street
North York, Ontario, Canada
M3H 5T6
Phone: 416/667-7710, Fax: 416/667-7799

SUMMARY

This report presents published LDEF micrometeoroid/debris impact data in a nomogram format useful for estimating the total number of hits that could be expected on a space structure as a function of time in orbit, angular location relative to ram and exposed surface area. Correction factors accounting for different altitudes are given, normalized to the average LDEF altitude. Examples on how to use the nomogram are also included. In addition, impact data and damage areas observed on composite laminates (experiment AO 180) are discussed.

ANALYSIS OF LDEF MICROMETEOROID/DEBRIS IMPACT DATA

From the individual LDEF experiment trays, tables of micrometeoroid/debris impact feature sizes were compiled in Ref. 1. This data was then summarized for each longitudinal panel to yield an angular (θ) distribution of total impacts around LDEF after 5.75 years in low Earth orbit. Figure 1 presents two distributions based on the "total" reported hits, and those hits which were $\geq$0.5 mm in size. It should be noted that the data shown are strictly valid only at $\theta = 0°, \pm30°, \pm60°, 90°, \pm120°, \pm150°, 180°$, and the curves cannot be integrated to give a total number of impacts.

Based on the number distribution presented in Fig. 1, it is possible to construct a general purpose nomogram which permits a user to estimate the total number of impacts on a satellite or component (at the LDEF nominal altitude and inclination) for any value of time in orbit, angular location around the satellite or space structure (constrained by $\theta_n = n \times 30°$ where n = 0, 1, 2, ... 12, corresponding to a 12-sided polygon model of the satellite or component), and exposed area. For example, Figure 2 presents the nomogram for LDEF based on a longitudinal panel area of ~10 m^2, assuming a nominal impact fluence of 300 impacts/m^2. The example panel shown in Fig. 2 corresponds to $\theta = 30°$. Thus the intersection of $\theta = 30°$ and the LDEF time in orbit axis (~5.75 years) yields an impact fluence of ~300 impacts/m^2. Following up along this constant fluence curve until one intersects the desired panel area (10 m^2), one can then translate horizontally across the graph to the "Number of Impacts" ordinate. For this example, one obtains $N \cong 3100$ which agrees with the number plotted in Fig. 1.

Using the LDEF data from Fig. 1, knowing panel areas and total time in orbit, one can construct a general purpose nomogram for varying areas of exposure and impact fluence levels as shown in Fig. 3. Once again it must be stressed that these curves can only be used to estimate the total number of impacts at discrete angles defined by $\theta_n = n \times 30°$, n = 0, 1, ..., 12, and are strictly valid for an LDEF average altitude of ~463 km and inclination of 28.5°. Later it will be shown how to correct these numbers for different altitudes and orbital inclinations.

EXAMPLES OF NOMOGRAM APPLICATIONS

The following examples are presented to illustrate how one can estimate the number of impacts on satellite elements using the nomogram of Fig. 3.

(a) LDEF Impacts at RAM Location — Check Case

Use the nomogram to estimate the number of impacts at $\theta = 0°$ for LDEF after 5.75 years in orbit, using a panel area of 10 m^2. Compare result with data in Fig. 1.

Figure 4 presents the solution for $\theta = 0°$ which yields $N_0 \approx 3{,}100$ impacts. From Fig. 1, one also obtains $N_0 \approx 3{,}100$ impacts.

(b) Circular Cylindrical Space Structure

Demonstrate the application of the 12-sided polygon model to estimate the angular distribution of impacts for a circular cylinder, 0.5 m in diameter, 10 m long, after 30 years in orbit.

(i) Panel Area (A)

$c = 2R \sin \phi$

For the 12-sided polygon $\phi = 15°$

$\therefore c = 0.13$ m and $A \equiv 1.3$ m^2

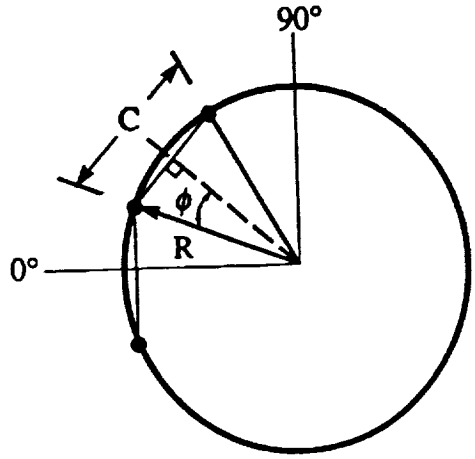

(ii) N_n Distribution from Fig. 3 (30 years)

θ_n^o	N_n (est.)	D_n* (cms)
0	2070	2.5
30	2070	2.5
60	1680	2.8
90	1100	3.4
120	450	5.4
150	325	6.3
180	290	6.7

θ_n^o	N_n (est.)	D_n* (cms)
-30	2260	2.4
-60	1680	2.8
-90	615	4.6
-120	550	4.9
-150	225	7.6

*Average impact feature separation distance on panel, assuming uniform distribution.

(c) Interpolation Example

If one wishes to use fewer than 12 sides to model a space structure, interpolation of the nomogram data must be employed. To demonstrate, consider the previous cylinder example. Let us replace the 12-sided polygon representation of the circular cross-section with the 6-sided model shown below.

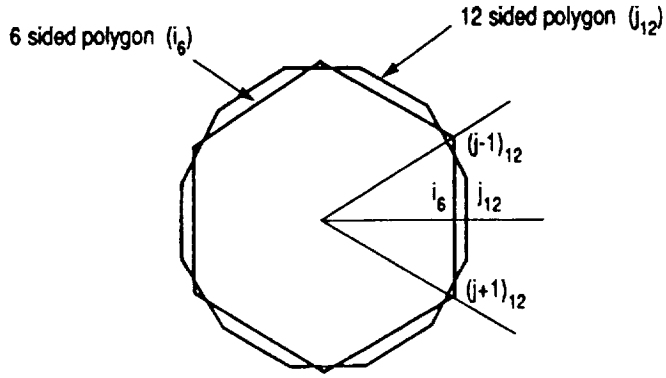

If one examines any panel i_6, for example, it is comprised of one facing j_{12} and half of each of the adjoining panels, denoted by $(j-1)_{12}$, $(j+1)_{12}$. Thus the number of impacts on this i_6 panel is given by,

$$N_{i_6} = \frac{1}{2}(N_{j-1_{12}} + 2N_{j_{12}} + N_{j+1_{12}})$$

For example, the panel (i=4) corresponding to $\theta = 180°$ on the reduced element model would sustain a number of impacts given by

$$N_{46} = \frac{1}{2}(325 + 2 \times 290 + 225)$$
$$= 565$$

A comparison of the impact number distribution is given below. Note that both "totals" must be equal.

θ_n	$N_{j_{12}}$	N_{i_6}
0°	2070	4235
30°	2070	—
60°	1680	3265
90°	1100	—
120°	450	1162.5
150°	325	—
180°	290	565
-150°	225	—
-120°	550	970
-90°	615	—
-60°	1680	3117.5
-30°	2260	—
Totals:	13315 =	13315

$$-\left(\frac{1}{2}N_{-30°} + N_{0°} + \frac{1}{2}N_{30°}\right)$$

$$-\left(\frac{1}{2}N_{30°} + N_{60°} + \frac{1}{2}N_{90°}\right)$$

$i_6 = 1, 2, ..., 6$

$j_{12} = 1, 2, ..., 12$

MODIFICATIONS OF NOMOGRAM DATA

(a) Micrometeoroid/Debris Impacts > 0.5 mm Diameter

For design purposes, it may be useful to know the number of impacts >0.5 mm in diameter and their angular distribution around a satellite. The figure shown below is based on the LDEF distribution plotted in Fig. 1 and provides a % allocation of the total number of hits attributable to this larger size category.

% distribution on each panel of micrometeoroid/debris impacts >0.5 mm based on LDEF data

θ_n	% N_n
0	9
30	8
60	13
90	10
120	17
150	6
180	9
-150	9
-120	5
-90	9
-60	8
-30	9

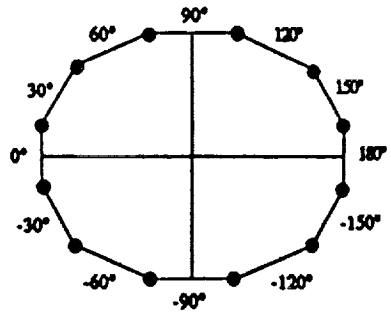

(b) Variation in Number of Hits with Altitude — Natural Micrometeoroid Environment

From Ref. 2, the flux of micrometeoroids in Earth orbit is given by

$$\phi = SF \cdot GE \cdot F^{ip}$$

where F^{ip} is the interplanetary flux,

SF is a shielding factor due to Earth's atmosphere,

GE is a factor which accounts for focussing by the Earth's gravity.

Again, Ref. 2 gives these factors as

$$SF = \frac{1 + \cos \eta}{2} \quad \text{where} \quad \sin \eta = \frac{R_e}{R_e + H} \quad \text{and} \quad GE = 1 + \frac{R_e}{r}$$

R_e represents the radius of Earth plus 100 km of atmosphere (= 6478 km), H the height above Earth's atmosphere, and r the orbit radius. Due to the considerable uncertainty in the physical properties of micrometeoroids, there is a 0.1 to 10 factor of uncertainty in the flux relationship.

However, one can determine the altitude dependence from

$$\frac{\phi}{F^{ip}} = \frac{1}{2}\left\{1 + \left[1 - \left(\frac{1}{1 + H/R_e}\right)^2\right]^{1/2}\right\}\left(1 + \frac{1}{1 + H/R_e}\right)$$

Assuming an average altitude for LDEF of ~463 km, then one can apply a correction factor to the nomogram data to account for flux changes with altitude. This factor is plotted in Fig. 5. Note that this correction must be applied to only the natural micrometeoroid component of the total number of hits recorded for LDEF.

(c) Variation in Number of Space Debris Hits with Altitude

From Ref. 2, the orbital debris model proposed is based on the assumption that the accumulation of objects in low Earth orbit is constant. One can derive a normalized debris flux ($\bar{\phi}_{OD}$) as a function of altitude (for $h \leq 2000$ km) having the form

$$\bar{\phi}_{OD} = \frac{\psi_i \phi(h, S)}{\phi(h, S) + 1}$$

where S represents a solar activity factor,
ψ_i is an inclination-dependent function = 0.91 for 28.5° (see Ref. 2 for table of ψ_i values),
and $\phi(h, S) = 10^{(h/200 - S/140 - 1.5)}$.

For particles with $d < 1$ cm, one can estimate an altitude correction factor that can be applied to the nomogram data, as shown in Fig. 5. Inclination correction factors can be found in Ref. 2.

It should be noted that at this point in time, the impact data for LDEF cannot be separated into "natural" or "debris" populations. Thus the individual correction factors shown in Fig. 5 cannot be applied. However, it is evident that for altitudes <400 km, one could use the debris correction factor, whereas at ≥400 km the micrometeoroid correction factor can be applied to all of the LDEF data derived from the nomogram to obtain conservative estimates.

MICROMETEOROID/DEBRIS IMPACTS ON EXPERIMENT AO180

Experiment AO180 consisted of various graphite, aramid and boron fiber-reinforced epoxy materials mounted at station D-12, about 82° from the LDEF velocity vector. The exposed surface area was ~0.6 m^2 and was subjected to a total of 84 hits (Fig. 6). The predicted number of impacts for this area after 5.75 years is ~80, based on the nomogram in Fig. 3 (assuming $\theta = 90°$). This agreement is particularly noteworthy since it demonstrates that after sufficient exposure time in orbit, one can predict the number of impacts likely to occur in relatively small areas.

From a detailed inspection of the composite samples (both tubes and flat plates), only 10 of the 84 hits were found on these materials, the balance located on end fixtures and the aluminum base plates.

MICROMETEOROID IMPACT ON ALUMINUM SUPPORT STRUCTURE

The largest impact (~1 mm diameter) found on experiment AO180 occurred on an aluminum base plate, with an ejecta splash observed on an adjacent flange structure (Fig. 7). SEM/EDX spectra of the crater rim material composition (Fig. 8) exhibited a strong Fe peak along with the Al substrate. Based on chemical composition evidence it is assumed that the crater resulted from debris impact. Figure 9 contains SEM photographs of the surface ejecta splash patterns on the flange structure. An aluminum ejecta particle, visible in Fig. 9, is enlarged in Fig.10. Figure 10 presents two different forms of aluminum ejecta particles and their associated splash patterns. The lower photograph shows the remnants of a molten particle while the upper photograph shows the full spherical form of an aluminum particle.

IMPACT DAMAGE ON COMPOSITE LAMINATES

Micrometeoroid/debris impacts on polymer matrix composites do not produce the typical hemispherical craters found on metallic structures. Rather, because of the brittle nature of the resin matrix, one generally finds penetration holes with adjacent surface damage, some internal ply delamination and local fiber fractures. For brittle fibers such as graphite, the impact and exit holes exhibit brittle fiber fractures as shown in Fig. 11, as well as rear surface spallation [5208/T300; $(\pm 45^\circ)_S$]. Note that the spallation damage-to-hole size ratio is about 5:1. On the other hand, tough non-brittle fibers such as aramid fail in a "brush or broom" mode surrounding the impact damage region. Figure 12 presents four impacts on a single Kevlar®/epoxy tube [SP-328, $(\pm 45)_{4S}$]. It can be seen that three penetrations occurred with one grazing (or low energy) impact that produced only local surface damage. Note the fiber failure mode in photo 4. From the enlargements, it was possible to scan the images to calculate the surface damage area and impact hole size. These images were digitized using a Houston Instruments "Hipad" digitizer to obtain an accurate reproduction of the impact site (~200 data points on average). The X-Y coordinates of the digitized photograph were then analysed using spreadsheet/graphics programs (Supercalc 5.0™ and Grapher™). A trapezoidal model was used to numerically integrate the digitized image to obtain damage area and crater size (assuming a circular hole). Figures 13, 14 and 15 present a summary of the images obtained for nine impact sites. At this point in time, only 10 impact sites (out of 84) have been found on the composite samples, a summary of which is given in Table 1 with estimates of surface damage area, hole size and penetration depth. Such data will be useful for estimating total damage on composite structures that arises from micrometeoroids/debris. Note that the penetration depth was based on the image enhanced backlighting technique, which is useful for translucent materials.

Using only the Kevlar®/epoxy impact data, one can construct a plot of surface damage area vs. major axis length, as shown in Fig. 16. It would appear that an elliptical model can be used to describe the damage area.

Figure 17 shows an SEM photomicrograph of the base of a crater (~0.076 mm^2 in area) in a Kevlar®/epoxy laminate (2T16) after the uppermost plies have been peeled off. An enlargement of a particle believed to have caused this crater is also shown (~10 μ in diameter). An SEM-EDX spectra is given in Fig. 18 where it can be seen that the debris particle is composed of Cr-Mn-Fe. Note that Al, Cu and Au come from the support fixtures holding the sample in the SEM.

REFERENCES

1. "Micrometeoroid and Orbital Debris Impact Features Documented on the Long Duration Exposure Facility — A Preliminary Report", LDEF SIG, NASA JSC, 1990.

2. Sisson, J: "Update of the Meteoroid and Orbital Debris Environment Definition," Space Station Level-II Change Request, CR #BB000883A.

Table 1. Summary of Impact Features on Composite Specimens (Experiment AO180)

Material Type	Sample Type	Number of Plies	Sample No.	Surface Damage Area (mm^2)	Hole Area (mm^2)	Nominal Hole Diameter (mm)	Particle Penetration Depth (Number of plies)
Graphite/Epoxy (T300/5208)	Plate	4		0.222	0.222		>4
Graphite/Epoxy (SP 288/T300)	Tube	4	1T10	1.064	0.083	0.325	>4
Aramid* Fiber/Epoxy (SP 328)	Tube	4	2T2	1.162	0.036	0.215	1~2
"	Tube	4	2T4	0.498	0.015	0.139	~1
"	Tube	4	2T11	0.423	0.018	0.152	~1
"	Tube	4	2T16	1.253	0.076	0.312	2~3
"	Tube	4	2T17(1)	0.223	—	—	1~2
			2T17(2)	1.445	0.033	0.204	2~3
			2T17(3)	0.370	—	—	~1
			2T17(4)	0.881	0.020	0.159	2~3

*Kevlar

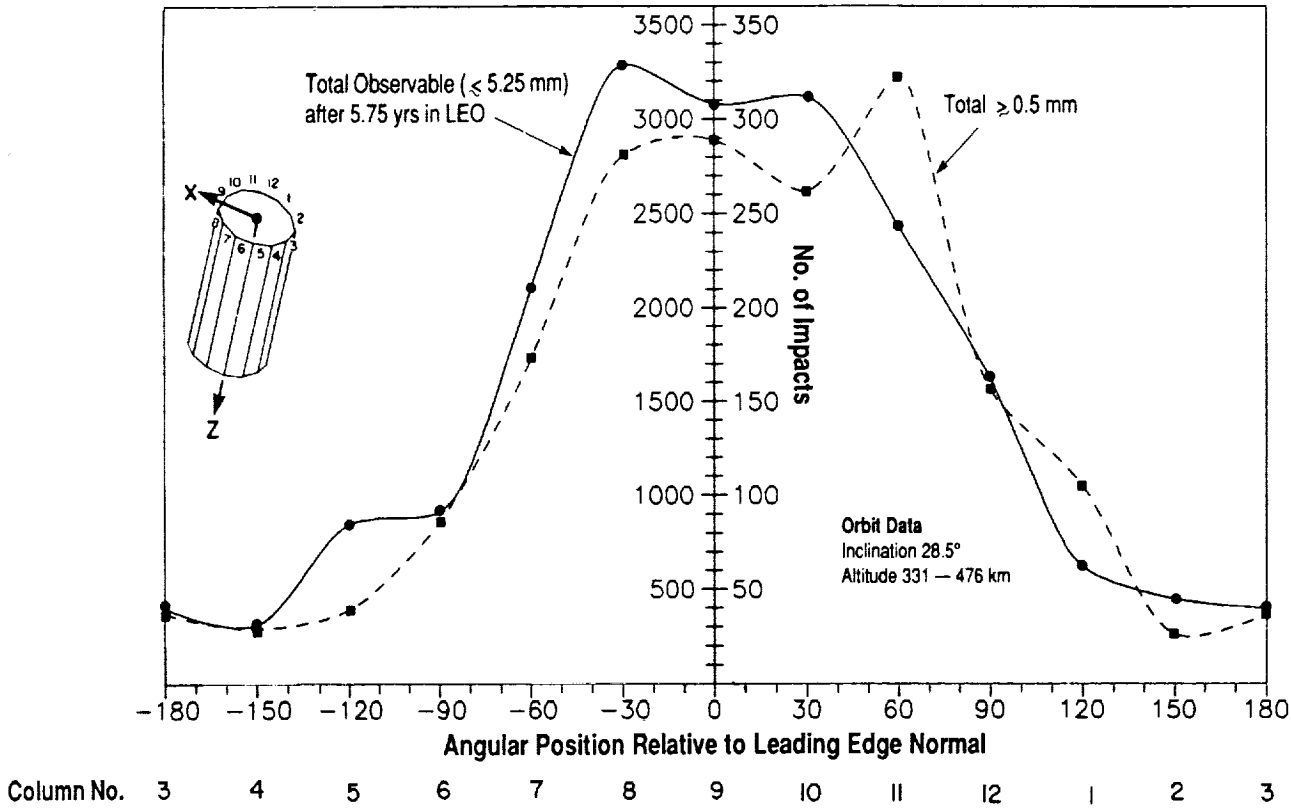

Figure 1. Circumferential distribution of micrometeoroid/debris impacts on LDEF (NASA M&D/SIG Report; Aug. 1990)

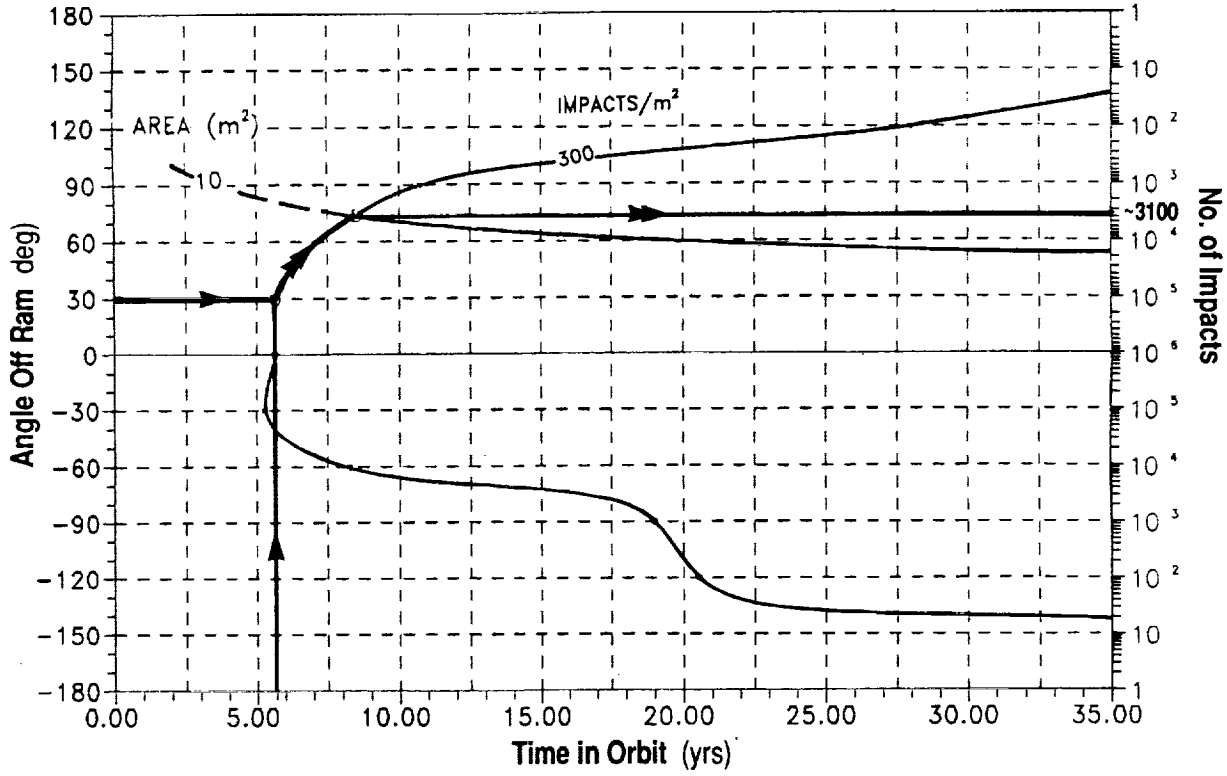

Figure 2. Nomogram for LDEF

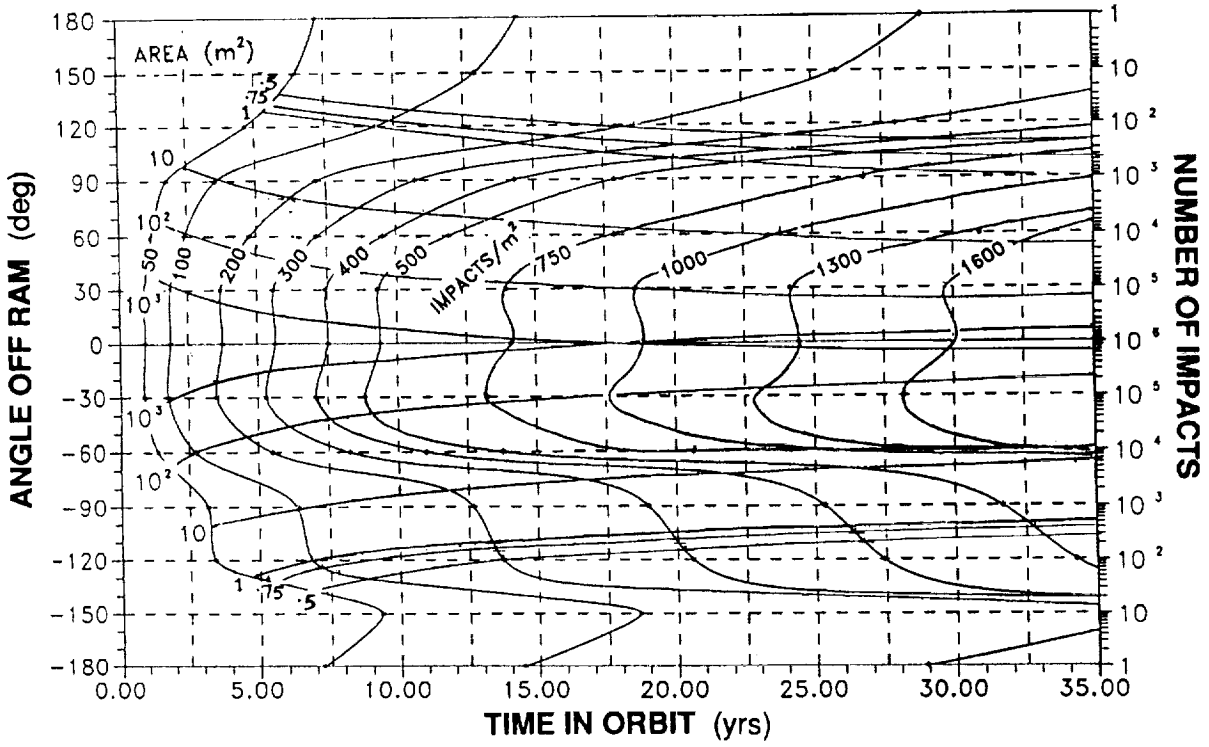

Figure 3. Nomogram for estimating total number of micrometeoroid/debris impacts for arbitrary exposed surface areas as a function of angle off ram and time in orbit

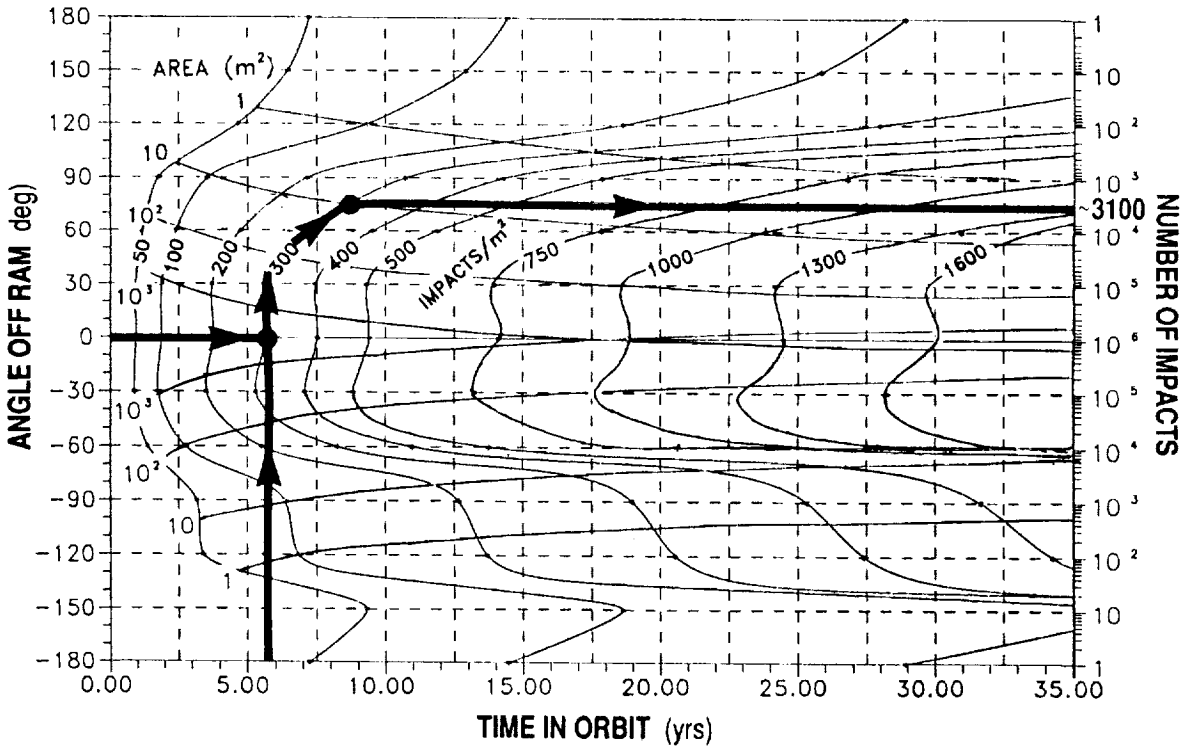

Figure 4.

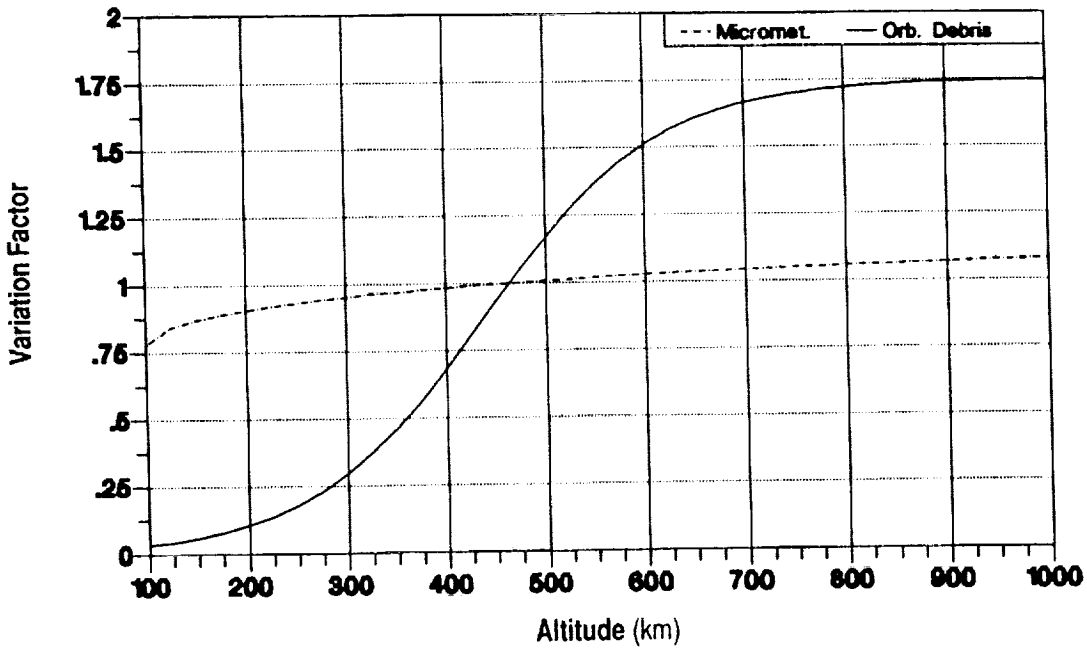

Figure 5. Normalized altitude variation factors (normalized to 464 km)
Note: orbital debris factors are for 1995 (projected)

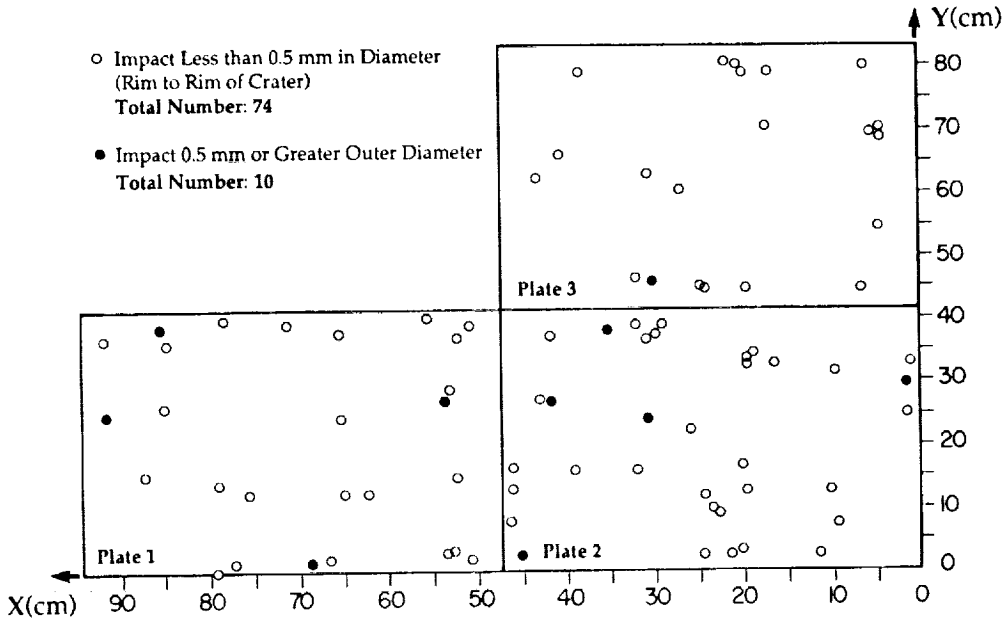

Figure 6. Micrometeoroid/debris impacts on UTIAS composite materials LDEF experiment (AO180, location D-12)

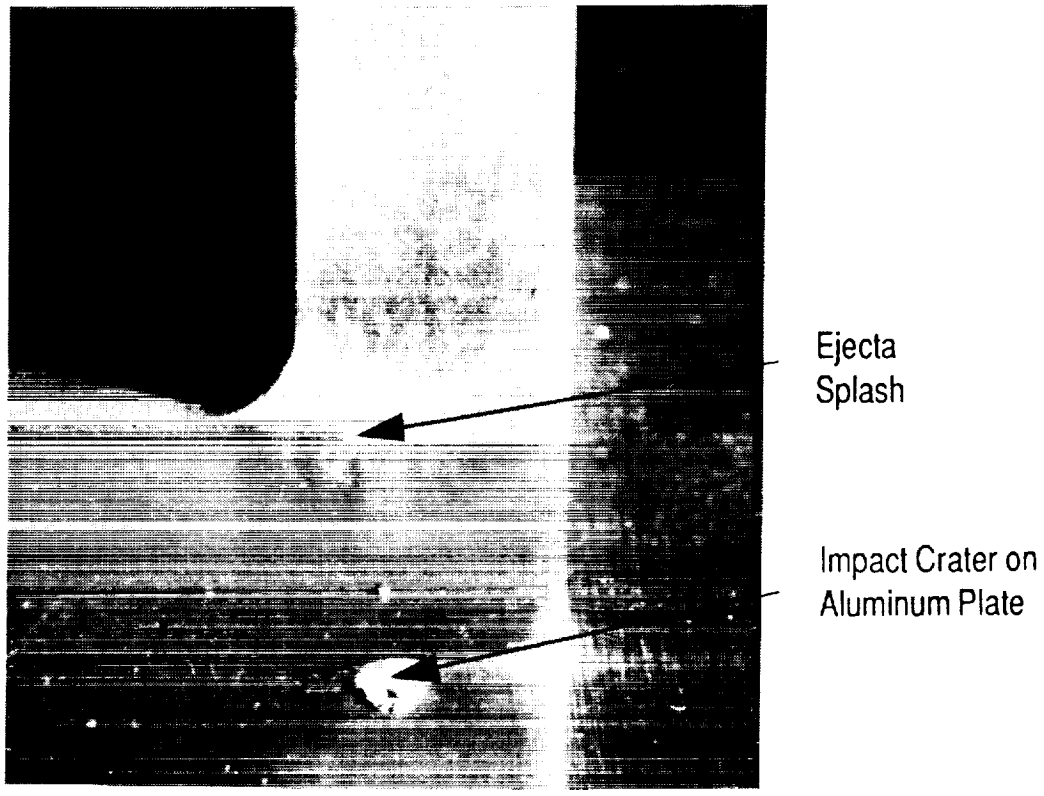

Figure 7. View of micrometeoroid impact crater and ejecta splash pattern on adjacent vertical flange structure

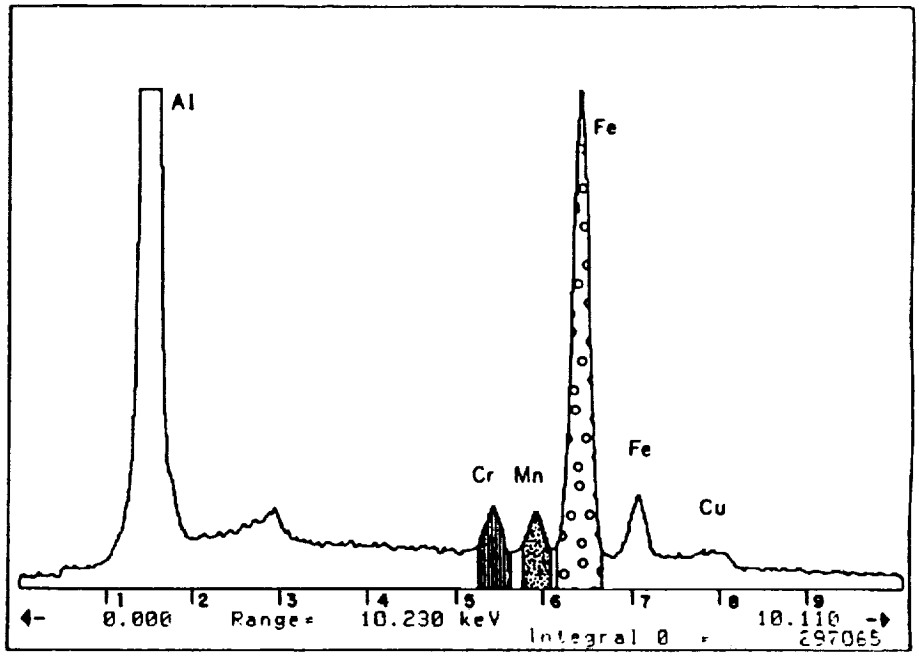

Figure 8. Crater ejecta and elemental composition (EDS spectra)

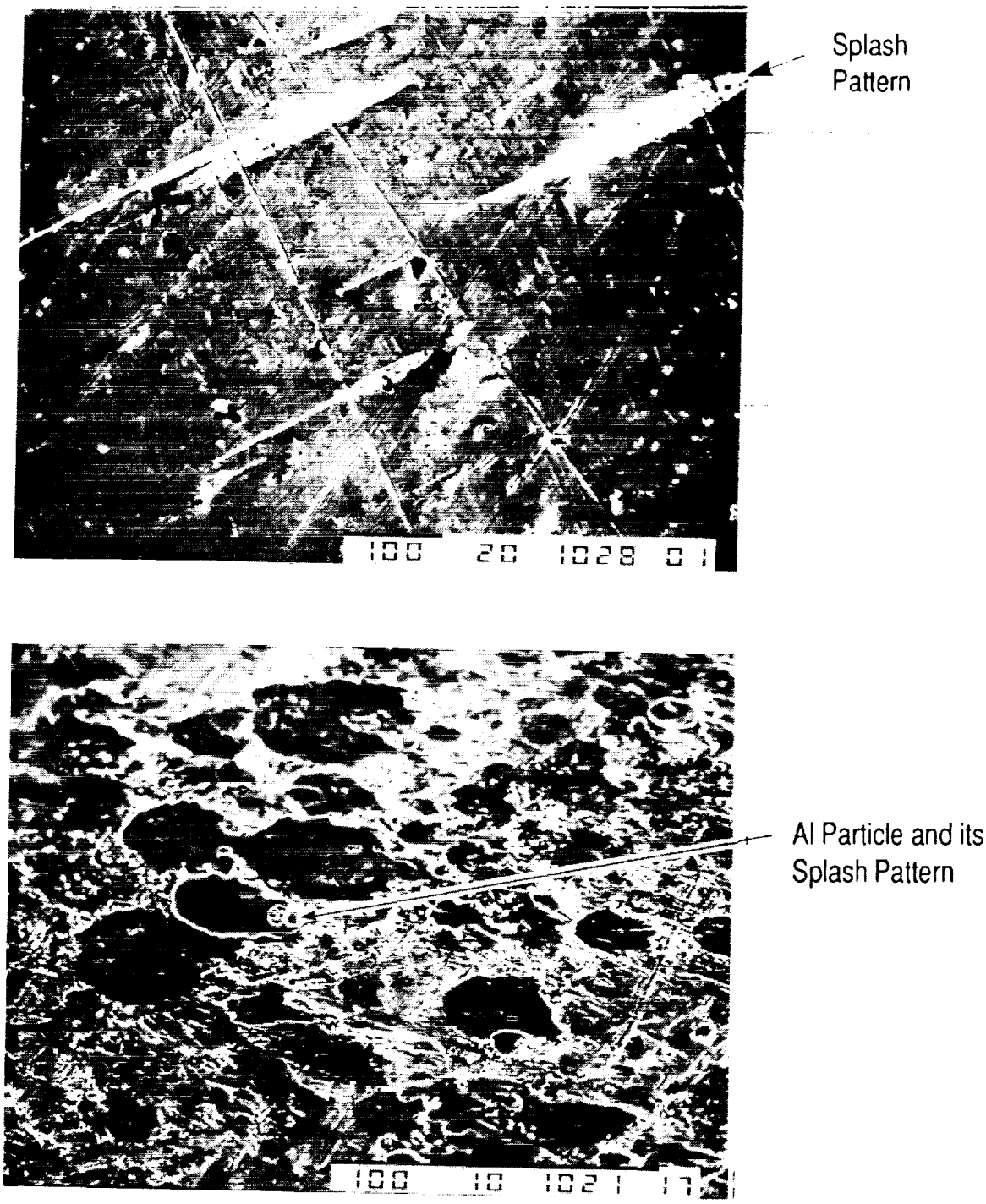

Figure 9. Different splash patterns formed by ejecta from micrometeoroid impact

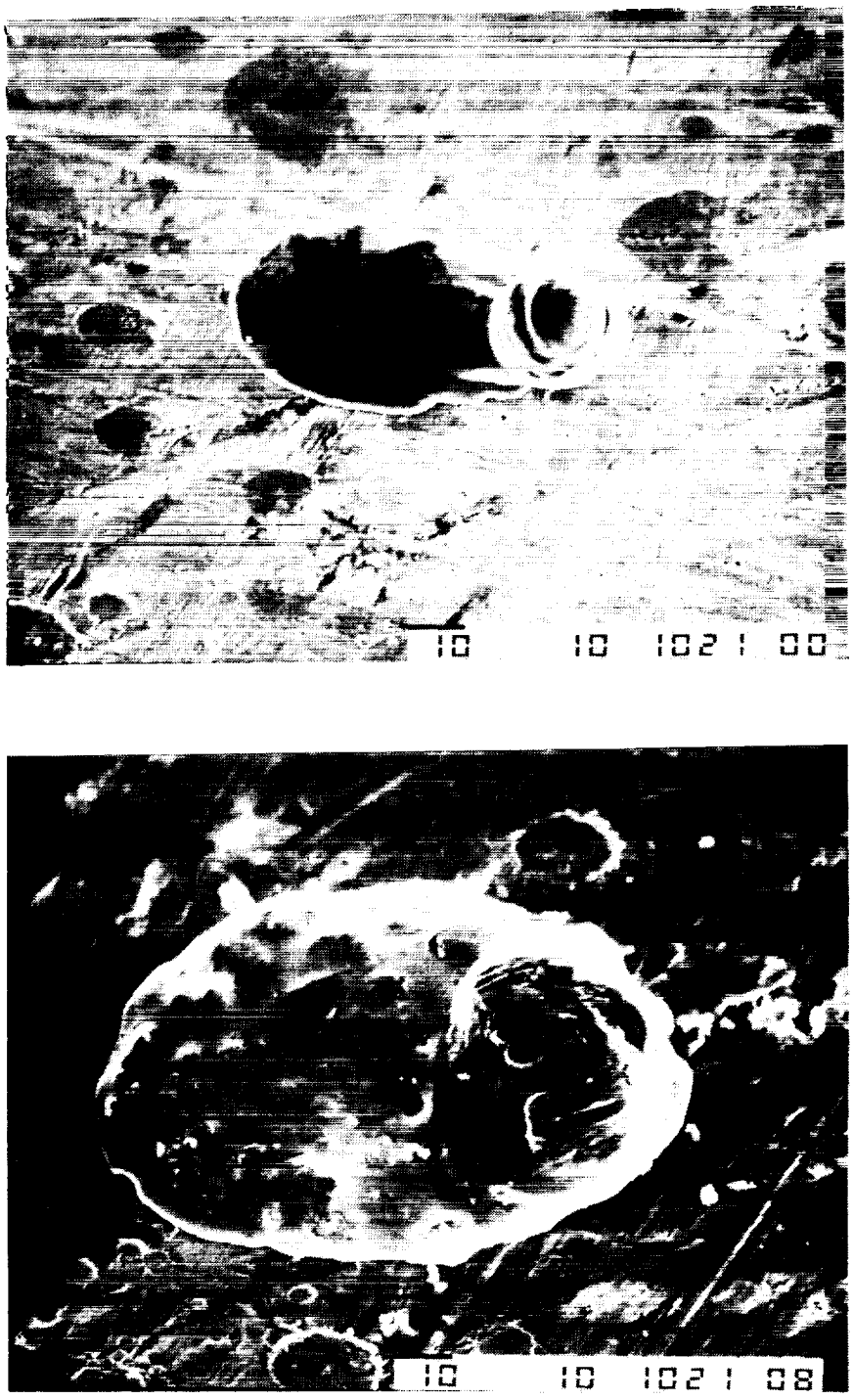

Figure 10. Aluminum ejecta particles with associated splash patterns

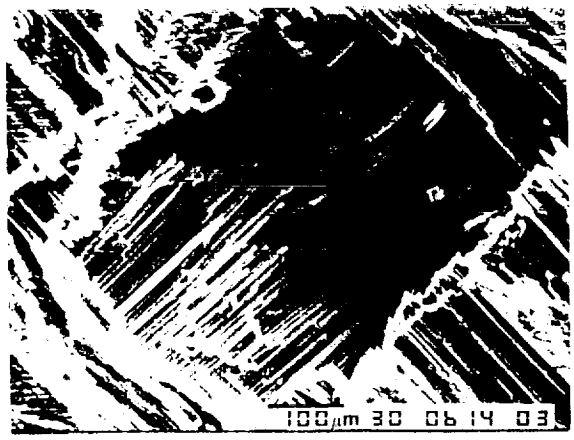

View of front face
impact hole (x100)

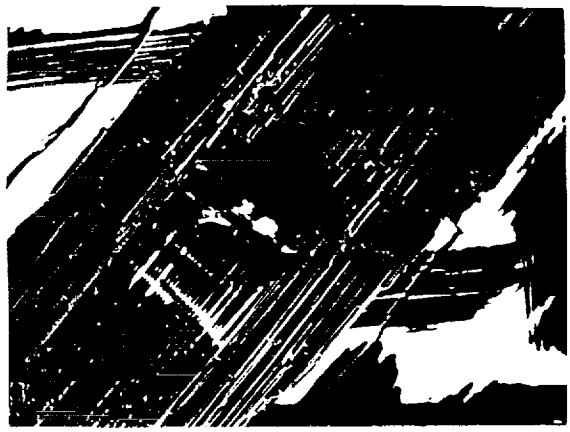

View of back face
exit hole (x100)

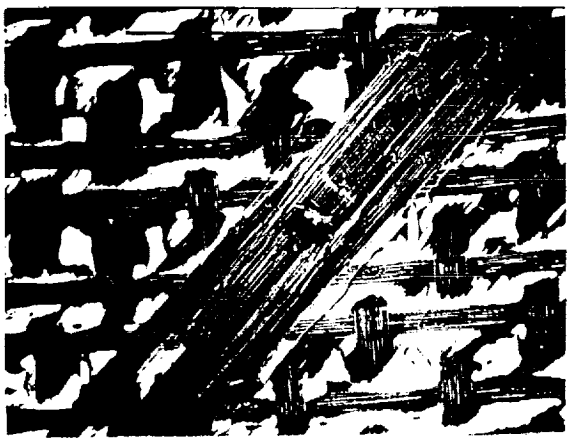

View of exit face damage
to composite laminate (x35)

Figure 11. SEM photographs of micrometeoroid/debris impact damage to graphite/epoxy laminate $(\pm 45^{\circ})_4$

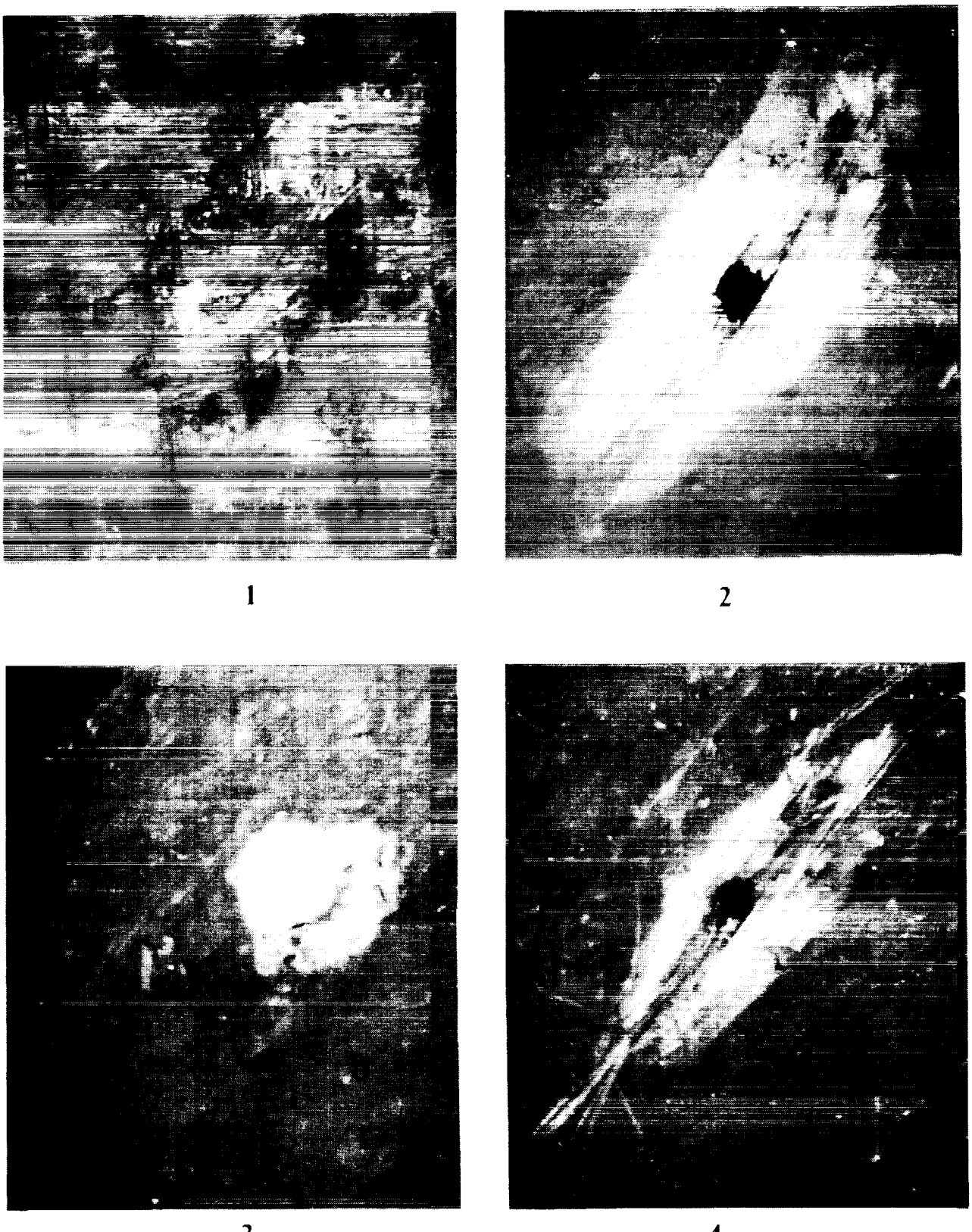

Figure 12. Micrometeoroid/debris impact damage (×100) on Kevlar®/epoxy tube [SP-328, $(\pm 45^{\circ})_{4S}$]

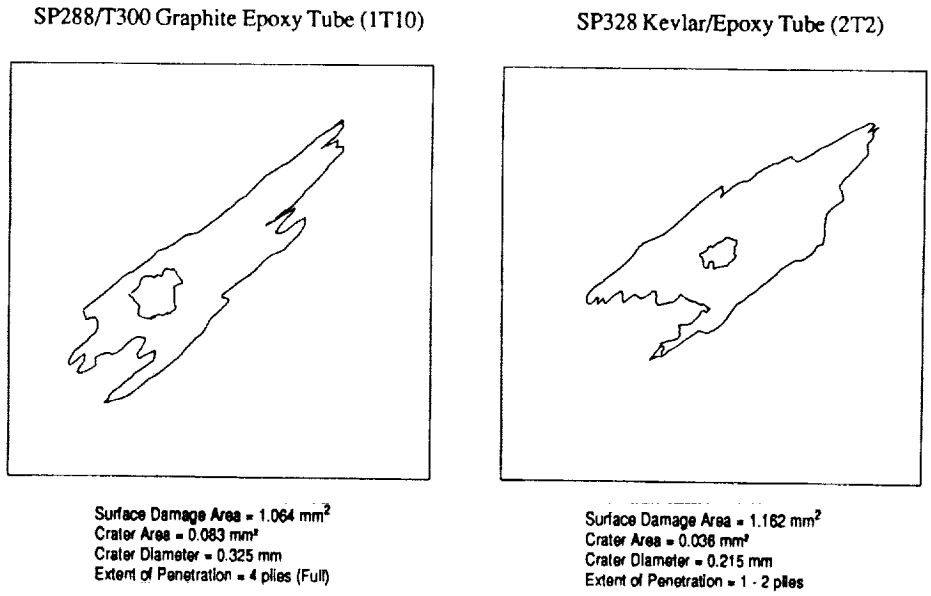

Figure 13. Micrometeoroid/debris impact damage

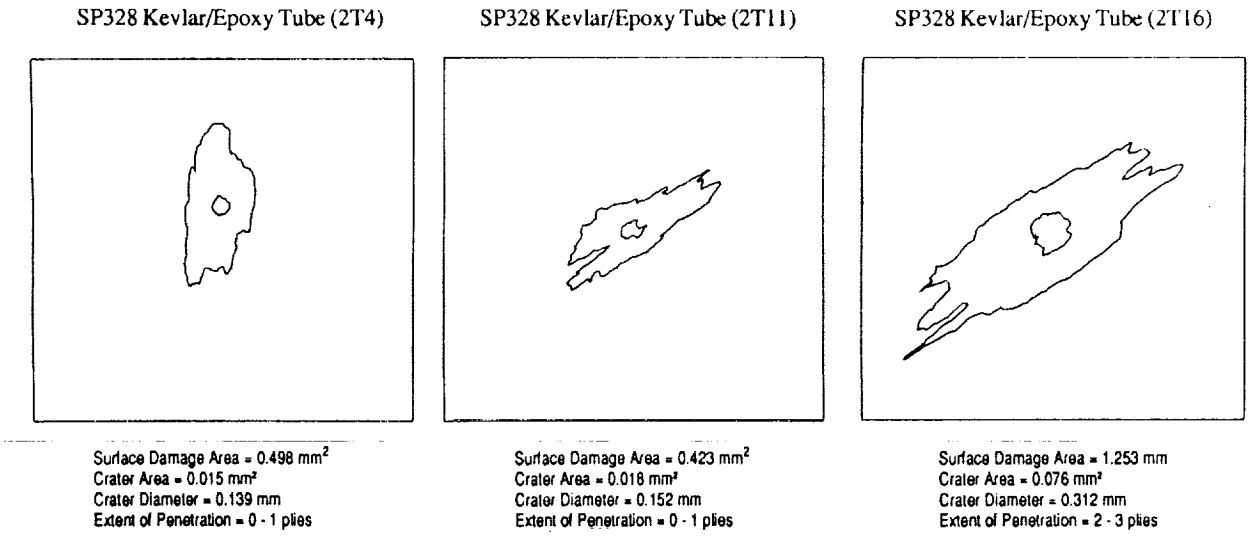

Figure 14. Micrometeoroid/debris impact damage

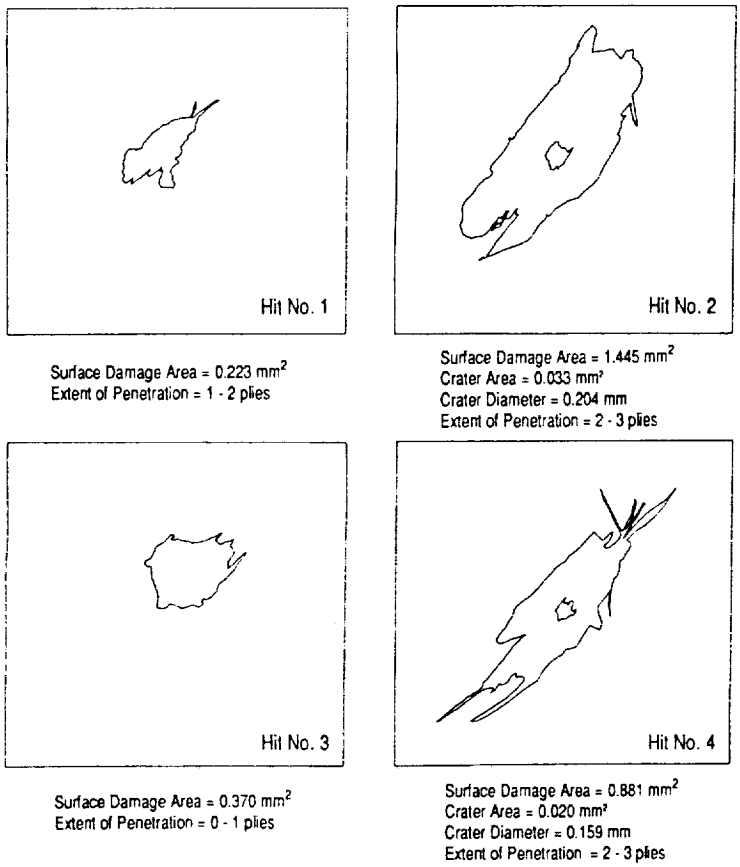

Figure 15. Micrometeoroid/debris impact damage, SP328 Kevlar®/epoxy tube (2T17)

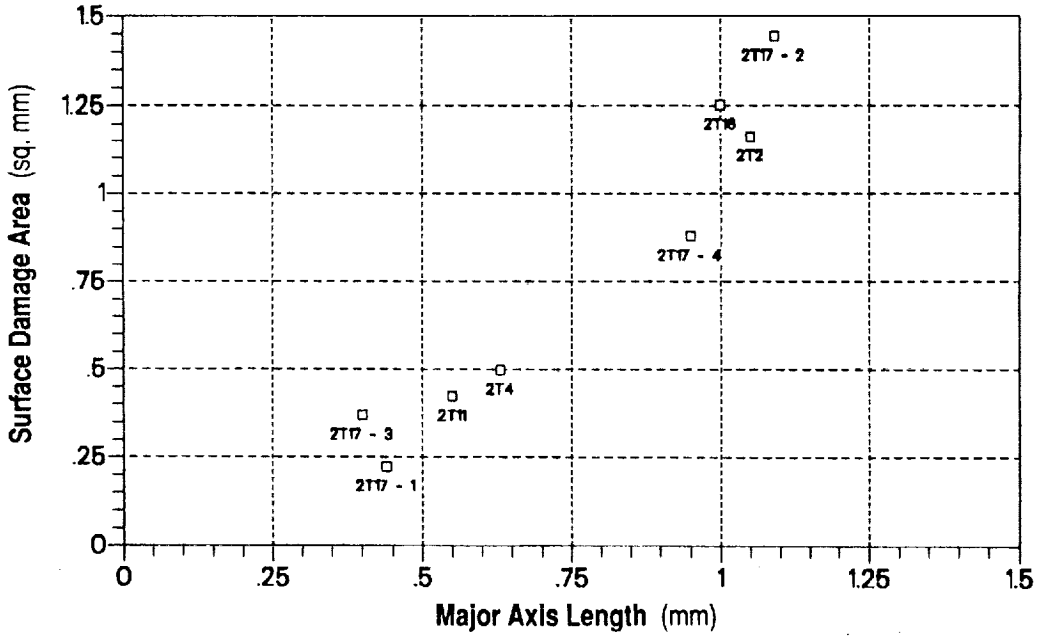

Figure 16

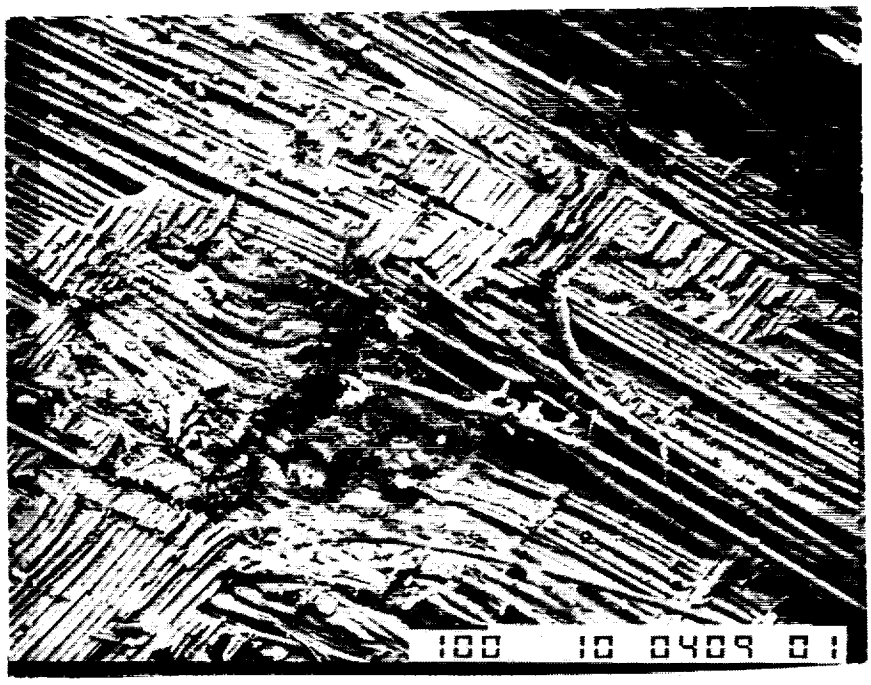

(a) Base of Impact Crater at 3rd Ply Interface

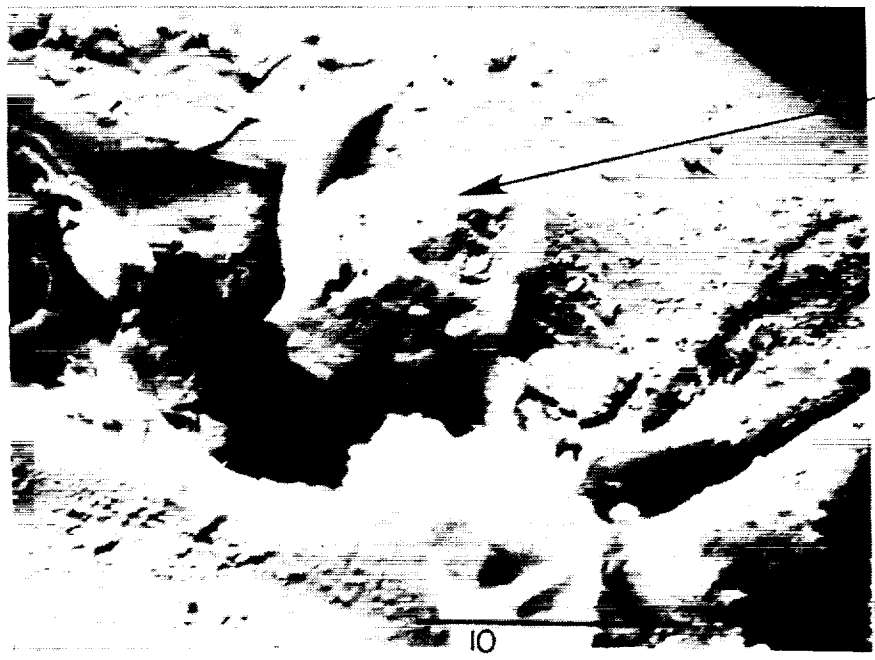

(b) Foreign Particulate in Crater

Figure 17. SEM photomicrographs of (a) impact crater base, and (b) particulate in crater for Kevlar®/epoxy tube (2T16)

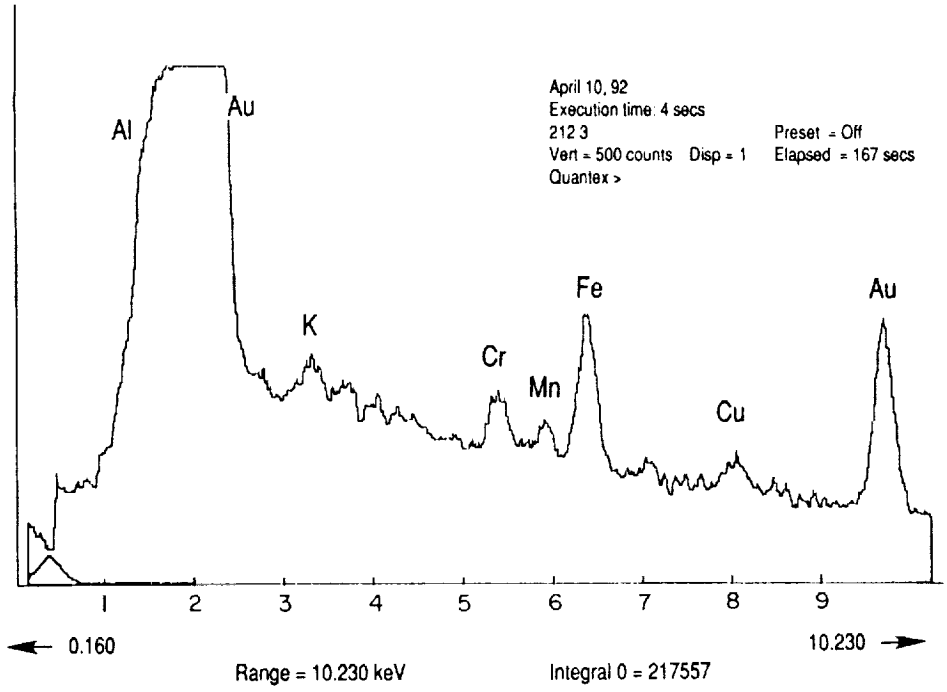

Figure 18. SEM-EDX spectra of particle in impact crater